CSIRO PUBLISHING

International Journal of Wildland Fire **2012**, *21*, 127–140
http://dx.doi.org/10.1071/WF10034

Entrainment regimes and flame characteristics of wildland fires

Ralph M. Nelson Jr[A,D], *Bret W. Butler*[B] *and David R. Weise*[C]

[A]US Forest Service, 206 Morning View Way, Leland, NC 28451, USA. [Retired]
[B]US Forest Service, Rocky Mountain Research Station, Missoula Fire Sciences Laboratory, Missoula, MT 59807, USA.
[C]US Forest Service, Pacific Southwest Research Station, Forest Fire Laboratory, Riverside, CA 92507, USA.
[D]Corresponding author. Email: nelsonsally@bellsouth.net

Abstract. This paper reports results from a study of the flame characteristics of 22 wind-aided pine litter fires in a laboratory wind tunnel and 32 field fires in southern rough and litter–grass fuels. Flame characteristic and fire behaviour data from these fires, simple theoretical flame models and regression techniques are used to determine whether the data support the derived models. When the data do not support the models, alternative models are developed. The experimental fires are used to evaluate entrainment constants and air/fuel mass ratios in the model equations. Both the models and the experimental data are consistent with recently reported computational fluid dynamics simulations that suggest the existence of buoyancy- and convection-controlled regimes of fire behaviour. The results also suggest these regimes are delimited by a critical value of Byram's convection number. Flame heights and air/fuel ratios behave similarly in the laboratory and field, but flame tilt angle relationships differ.

Additional keywords: air/fuel mass ratio, combustion regimes, entrainment constant, flame height, flame tilt angle.

Received 18 March 2010, accepted 23 February 2011, published online 24 November 2011

Introduction

An important aspect of wildland fire behaviour deals with whether a surface fire will transition to crown fire, and if so, which type of crown fire will develop (Tachajapong *et al.* 2008; Cruz and Alexander 2010). The size and shape of the flames are significant factors in this transition because of their influence on important processes such as heat transfer to unburned fuel, scorching of trees, sustained fire due to breaching of firebreaks and fire spread in discontinuous fuels (Lozano *et al.* 2010).

Flame characteristics have been studied in laboratory tests (Thomas *et al.* 1963; Thomas 1964; Van Wagner 1968; Fang 1969; Albini 1981; Nelson and Adkins 1986; Fendell *et al.* 1990; Weise and Biging 1996; Mendes-Lopes *et al.* 2003; Sun *et al.* 2006) and experimental field fires (Byram 1959; Thomas 1967; Nelson 1980; Nelson and Adkins 1988; Burrows 1994; Fernandes *et al.* 2002). Alexander (1998) used results from Fendell *et al.* (1990) to derive a relationship for fire plume angle from fireline intensity and wind speed in the development of a model to predict crown fire initiation. Anderson *et al.* (2006) tested currently available flame characteristic models with data from several sources and pointed out the need for standardised measurement methods.

The flame geometry of 2-D wildland fires has been simulated with computational fluid dynamics (CFD). For example, flame characteristics predicted by Porterie *et al.* (2000) compared favourably with flame models in the literature. Morvan and Dupuy (2004) related heat transfer and fire spread rate in Mediterranean shrub to a flame-length Froude number. Nmira *et al.* (2010) describe a physical model that produced low- and high-wind regimes of flame characteristic behaviour for stationary area and line fires; predicted values of flame height, flame length and flame tilt angle generally agreed with experimental data. Modelling studies of air flow around fires were reported for laboratory chaparral fires (Zhou *et al.* 2005; Lozano *et al.* 2010) and for grass fires in the field by Linn and Cunningham (2005).

Past research has essentially neglected the processes governing movement of air into the fuel-bed combustion zone and its attached flame. We know of only one published report in which the flame air/fuel mass ratio is estimated from air flow measurements; the laboratory data are for fires in alcohol, wood crib and town gas fuels (Thomas *et al.* 1965). Wildland fire models characterising entrainment are those of Thomas (1963), Fang (1969) and Albini (1981). In the present paper, models of entrainment and flame characteristics are basically thermodynamic, and restricted to head fires of low-to-moderate intensity on flat ground.

Numerical simulations (Porterie *et al.* 2000; Morvan 2007) suggest that a line of fire spreading in uniform fuel in response to a steady wind may burn in one of several combustion regimes. These regimes are related in part to the processes by which air is entrained into the flame. We hypothesise that when the mean wind speed is zero, the mass of entrained air increases as flame height increases and the velocity of this air at a given height is proportional to the upward velocity of the flame fluid at that point (Taylor 1961; Thomas 1967; Fleeter *et al.* 1984). This process is herein referred to as *classical entrainment*.

As the wind speed increases, convection begins to influence entrainment; flame tilt angle and rate of fire spread begin to increase significantly, and the flame height to depth ratio begins to decrease. The angle of flame tilt is determined by a momentum flux balance between the transverse components of the horizontally moving ambient air and the buoyant velocity of the flame fluid. This type of entrainment, associated with flame drag and buoyancy forces, is called *dynamic entrainment* in this paper.

As the wind continues to increase, a point is reached beyond which the mass of air entering the flame disrupts the balance between drag and buoyancy forces. The tilt angle is determined by a ratio between the horizontal and vertical components of the flame fluid mass flux (Albini 1981). This process is referred to in the present paper as *accretive entrainment.* In some cases of accretion, there may be little suggestion of horizontal inflow at the lee edge of the flame because part of the impinging air flows through the flame, leading to an outflow of unreacted air (air not participating in combustion) at the lee edge. Beer (1991) reported that CSIRO (Australia) researchers did not observe a fire-induced wind in their laboratory and field experimental fires.

The objective of this paper is to describe with mathematical models and experimental data how air entrainment and combustion regimes determine flame characteristics; we use models of flame height and tilt angle to evaluate entrainment constants and air/fuel mass ratios. First, we estimate air/fuel ratios for the combustion zone and flame. Second, we derive a dimensionless criterion that identifies three combustion regimes for head fires of low-to-moderate intensity. Third, we describe mass flow in the combustion zone and then develop flame characteristic equations from a 1-D analysis based on a simplified version of the Albini (1981) flame model. The present study extends Albini's work with formulations of flame characteristic equations and entrainment velocity for low-wind fires. Finally, we perform regressions using the model equations and experimental data to determine air/fuel ratios for the combustion zone and flame.

Combustion regimes

Evidence for multiple regimes

Albini (1981) stated that his flame model must fail at low wind speeds. In his model, the entrainment velocity is proportional to the horizontal wind speed. Porterie *et al.* (2000) simulated the laboratory pine litter fires of Mendes-Lopes *et al.* (1998) and reported that as wind speed increases from 1 to $2\,\mathrm{m\,s^{-1}}$, a transition from buoyancy-dominated to wind-dominated flow occurs. Beer (1993) observed differing functional relationships between fire spread rates and wind speed at a critical speed of $2.5\,\mathrm{m\,s^{-1}}$. Roberts (1979) used dimensional analysis to describe flow of effluent from a line of ocean outfall diffusers into a current of ambient water. These long pipeline diffusers have uniformly spaced ports through which effluent is forced by the water head. Dilution of the buoyant wastefield is closely approximated by treating the effluent source as a line plume (Roberts *et al.* 1989). When applied to wildland fires, the work of Roberts suggests that if differing head fire burning regimes are related to mixing differences, these regimes can be described in terms of wind speed and fireline intensity.

A combustion regime criterion

We utilise the work of Roberts (1979) on the basis that low-Reynolds-number ocean flows should provide a more realistic analogy for describing our low-Reynolds-number flames than models from other disciplines – for example, turbulent atmospheric plume models. When effluent issues vertically from a line diffuser into horizontally moving ocean water, the density difference between effluent and water induces a buoyancy flux that interacts with the water (Roberts 1979). This scenario differs from that for the wind-aided 2-D fire in at least two ways: (1) the flame may be more strongly buoyant than the effluent plume; (2) diffusers are straight, but wind-aided fires often exhibit one or more heads. We neglect these differences in the present study. For convenience of the reader, the 'Symbols used in mathematical models' section presents a list of symbols used in the mathematical modelling that follows.

The buoyancy flux per unit length of diffuser introduced by Roberts (1979) is

$$b_R = \frac{g\Delta\rho q}{\rho_e} \tag{1}$$

with units of cubic metres per second cubed. The corresponding buoyancy flux b_F for a line fire is

$$b_F = \frac{\phi_f g I_B}{\rho_a H_c} = \frac{g I_B}{\rho_a c_p T_a} = \frac{u_a^3 N_c}{2} \tag{2}$$

where the first equality of Eqn 2 is obtained by analogy with Eqn 1 and ϕ_f is the mean air/fuel ratio (mass of air per mass of original fuel burned) associated with lateral movement of air into the flame. The N_c criterion is

$$N_c = \frac{2 g I_B}{\rho_a c_p T_a u_a^3} \tag{3}$$

and often is called the convection number (Nelson 1993). In Eqn 3, we assume that ambient wind speed (u_a) is much greater than the fire spread rate. For a given ocean current of speed (u_c), Roberts defines a Froude number (F_R) as

$$F_R = \frac{u_c^3}{b_R} \tag{4}$$

and discusses three separate mixing regimes delineated by F_R. For $F_R < 0.2$, the flow forms a plume with a strong vertical component. In the intermediate region, $0.2 < F_R < 1$ and the plume is unable to contain all of the incoming flow; it contacts the lower boundary for some distance downstream. For $F_R > 1$, the flow is in full contact with the lower boundary and the upper edge of the plume forms a planar interface with ocean water. If similar behaviour occurs when a 2-D fire burns in air of horizontal speed u_a, then a fire Froude number (F_F) may be obtained from Eqns 2 as

$$F_F = \frac{u_a^3}{b_F} = 2N_c^{-1} \quad (5)$$

We apply the F_R criteria identified by Roberts (1979) to F_F so that three combustion regimes are defined by the critical values $N_c = 2$ and 10. For a given fireline intensity, the region $N_c > 10$ should correspond to weak wind speeds, whereas $N_c < 2$ would imply strong winds; the intermediate regime should apply to moderate winds.

A theoretical air/fuel mass ratio ϕ_f for the free flame may be obtained from Eqns 2. If $H_c = 15\,000\,\text{kJ kg}^{-1}$, $c_P = 1\,\text{kJ kg}^{-1}\,\text{K}^{-1}$ and $T_a = 300\,\text{K}$, then

$$\phi_f = \frac{H_c}{c_p T_a} = 50 \quad (6)$$

with units of kilogram per kilogram. Support for Eqn 6 comes from the following considerations. Byram and Nelson (1974) found that the steady burning of 1 kg of solid wood expands the atmosphere by $41.8\,\text{m}^3$. Suppose a mixture of combustion products and unreacted air at mean temperature $T_o = 1000\,\text{K}$ enters the flame from the combustion zone along with air entrained laterally from the atmosphere at temperature $T_a = 300\,\text{K}$. Mass M_e of the entrained air has initial volume V_o and receives heat from the combustion zone fluid. Thus M_e expands to a larger volume V, causing a drop in the mean temperature of the fluid. The mixture of combustion products and entrained air exits the flame tip at temperature $T_t = 500\,\text{K}$. If the atmospheric density is $1.2\,\text{kg m}^{-3}$ and air flows in steadily to replace all air leaving the visible flame volume, then the effective air/fuel mass ratio is $\phi_f = (1.2 \times 41.8) = 50.2$ kg air kg^{-1} fuel burned, in agreement with Eqn 6.

Theory of flame characteristics

Consider a line head fire that burns steadily in response to horizontal wind speed u_a through fuel distributed uniformly on flat terrain. Modelling of entrainment and flame characteristics requires consideration of both the combustion and flame zones; the overall rates of mass flow associated with these zones are derived below.

Combustion zone relationships

The mixture flowing into the flame consists of burned and unburned volatiles, reacted air (air participating in combustion), unreacted air, water vapour formed in combustion, and water not lost during fuel preheating. An approximate mass flow rate through the fuel bed surface per unit length of fireline, m_o ($\text{kg m}^{-1}\,\text{s}^{-1}$), is

$$m_o = X_b W_a R\left[\frac{1}{X_b} + N_v + \frac{Z}{\varepsilon X_b} + 0.56 + \frac{fM}{\varepsilon X_b}\right] \quad (7)$$

where X_b is the fraction of volatilised fuel that burns. From left to right, the terms in brackets denote the mass of volatiles produced in the combustion zone, air (reacted and unreacted) present in the combustion zone, and water released from the fuel owing to combustion and evaporation. Thus Eqn 7 describes the stream of combustion products, unreacted air and water vapour entering the flame from the combustion zone.

Fireline intensity is defined as

$$I_B = H_c X_b W_a R \quad (8)$$

where X_b is now interpreted as the ratio of the heat release rate I_{Bcz} in the combustion zone to the heat release rate I_B of the entire fire. When $X_b = 1$, Eqn 8 agrees with the widely accepted definition of fireline intensity, $I_B = H_c W_a R$.

A different approximation of I_B calculates the heat required to raise the temperature of the fluid entering the base of the flame from ambient temperature (i.e. before the production of heat by chemical reaction) to the mean temperature at the base of the flame (Albini *et al.* 1995). Thus when $X_b = 1$, I_B may be written as

$$I_B = m_o c_p (T_o - T_a) \quad (9)$$

where c_p is assumed equal for flame fluid and air. In the combustion zone of a wildland fire, $X_b < 1$ and the rate of heat release, from Eqns 7–9, is

$$\begin{aligned} I_{Bcz} = H_c X_b W_a R = X_b W_a R\left[\frac{1}{X_b} + N_v + \frac{Z}{\varepsilon X_b} + 0.56 + \frac{fM}{\varepsilon X_b}\right] \\ \times c_p(T_o - T_a) \approx X_b W_a R\left[\frac{1}{X_b} + \phi_{cz}\right] c_p (T_o - T_a) \end{aligned} \quad (10)$$

where ϕ_{cz} is the air/fuel ratio of the combustion zone given by the sum of N_v kg of reacted air and $Z/\varepsilon X_b$ kg of unreacted air. If the simplified estimate of I_{Bcz} in Eqn 10 is reasonable, ϕ_{cz} becomes

$$\phi_{cz} = \frac{H_c}{c_p(T_o - T_a)} - \frac{1}{X_b} \approx 20 \quad (11)$$

When X_b ranges from 0.5 to 1, ϕ_{cz} ranges from 19.4 to $20.4\,\text{kg kg}^{-1}$ and a mean theoretical ϕ_{cz} may be taken as $20\,\text{kg kg}^{-1}$.

The approximation in Eqn 10 requires $(1/X_b + \phi_{cz}) >> (0.56 + fM/\varepsilon X_b)$; we make the reasonable assumptions $\varepsilon > 0.5$ and $X_b > 0.5$ (Albini 1980). For the ordinary laboratory fire $(0.56 + fM/\varepsilon X_b) < 2$, so Eqn 10 is acceptable. For the green vegetation layers of crown fires, the estimate is less accurate because the moisture term $(0.56 + fM/\varepsilon X_b)$ could be as large as 9.

Flame zone relationships

In the Albini (1981) flame model, air enters the flame by accretion, in which a fraction of the impinging air of speed u_a becomes incorporated into the flame. Because chemical reactions are neglected in our model, flame temperature is a maximum at the fuel bed surface and decreases upward as air entrainment increases towards the flame tip.

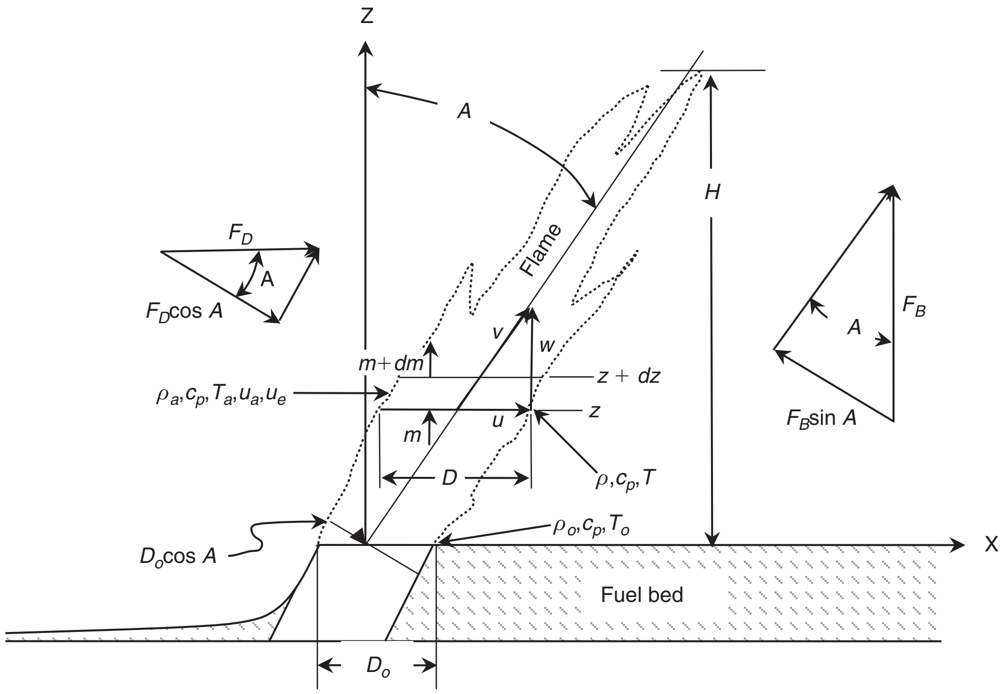

Fig. 1. A time-averaged visible flame showing mass and energy flow variables. The transverse component of the horizontal drag force F_D balances the transverse component of the vertical buoyancy force F_B to determine flame tilt angle A.

We rewrite the Albini (1981) model equations as follows:

$$\text{mass flow:}\ m = \rho w D \tag{12a}$$

$$\text{lateral entrainment:}\ dm = \rho_a u_e dz \tag{12b}$$

$$\text{horizontal momentum:}\ d(mu) = u_a dm \tag{12c}$$

$$\text{vertical momentum:}\ d(mw) = \rho g D\left[\frac{(T - T_a)}{T_a}\right]dz \tag{12d}$$

$$\text{sensible energy:}\ d(mc_pT) = c_pT_a dm \tag{12e}$$

$$\text{flame tilt angle:}\ A = \tan^{-1}\left(\frac{u}{w}\right) \tag{12f}$$

The flame represented by Eqns 12a–f is presented in Fig. 1. All dependent variables in these equations are regarded as time-averaged values.

Eqns 12a–f may be solved analytically by assuming that entrainment velocity u_e represents a constant velocity obtained by averaging over flame height H. Quantities ρ_a, c_p, T_a and u_a are assumed constant. When the entrainment and sensible energy relations Eqns 12b and 12e are integrated from the flame base ($z = 0$) to the flame tip ($z = H$), the flame tip mass flux (m_t) becomes

$$m_t = m_o\frac{(T_o - T_a)}{(T_f - T_a)} = m_o + \rho_a u_e H \tag{13}$$

where m_o ($= \rho_o w_o D_o$) is the combustion zone mass flux at $z = 0$. If values of 1000, 500 and 300 K are assigned to T_o, T_t and T_a, then $m_t = 3.5m_o$ and Eqns 10 and 13 give

$$\rho_a u_e H = 2.5m_o = 2.5(1 + X_b\phi_{cz})W_aR = \phi_f X_b W_a R = \frac{\phi_f X_b I_B}{H_c} \tag{14}$$

where X_b may be taken as unity.

The horizontal momentum equation is integrated with limits $u = u_o$ and $m = m_o$ when $z = 0$ to obtain

$$mu = m_o u_o + u_a(m - m_o) \tag{15}$$

The vertical momentum equation may be rewritten by multiplying both sides by mw and substituting the entrainment and integrated sensible energy equations to obtain

$$d(mw)^2 = \left[\frac{2gm_o}{\rho_a u_e}\right]\left[\frac{c_p(T_o - T_a)}{c_pT_a}\right]dm^2 = \left[\frac{2gI_B}{\rho_a c_p T_a u_e}\right]dm^2 \tag{16}$$

where I_B is from Eqn 9. Integration of Eqn 16 with $(mw)^2 = (m_o w_o)^2$ at $z = 0$ leads to

$$(mw)^2 = (m_o w_o)^2 + \frac{w_c^3}{2u_e}\left(m^2 - m_o^2\right) \tag{17}$$

where the quantity w_c is a characteristic buoyant velocity (Nelson 2003) representative of the whole fire given by

$$w_c = \left(\frac{2gI_B}{\rho_a c_p T_a}\right)^{1/3} \tag{18}$$

Boundary velocities u_o and w_o depend strongly on wind speed, fuel type and fuel load. Anderson *et al.* (2010) have shown that at higher speeds, u_o is a moderate fraction of the free stream speed u_a; for small u_a values, u_o ranges from u_a to $2u_a$. However, w_o is instrumental in the development of model equations for flame height H and tangent of the tilt angle, tan A.

Entrainment velocity equations

Albini (1981) assumed that entrainment velocities for head fires in moderate winds can be described as

$$u_e = \eta u_a \tag{19}$$

where η is the fraction of impinging air entering the flame. Because Eqn 19 is not valid as u_a approaches zero, we require an expression for u_e in terms of entrainment constant α that is applicable for $u_a \geq 0$. On the basis of exploratory data plots (R. M. Nelson Jr, Missoula Fire Sciences Laboratory, unpubl. data), and because w_c in Eqn 18 is proportional to $I_B^{1/3}$ (a function of W_a and u_a), we infer

$$u_e = \alpha w_c \tag{20}$$

an equation identical in form to the zero-wind entrainment equation (Taylor 1961). For single fires, Eqn 20 applies when $u_a > 0$; the equation $u_e = \alpha_o w_{co}$ applies when $u_a = 0$. In general, we expect $\alpha \neq \alpha_o$. Entrainment constants η and α are quantified in the next section, which compares flame characteristic model equations with our experimental data.

Flame tilt angle relationships

The tangent of flame tilt angle A may be obtained from Eqn 15 and the square root of Eqn 17 in the form

$$\tan A = \frac{u}{w} = \frac{[m_o u_o + u_a(m - m_o)]}{\left[(m_o w_o)^2 + w_c^3(m^2 - m_o^2)/2u_e\right]^{1/2}} \tag{21}$$

If we invoke the assumptions used by Albini (1981) and assume little variation in angle A from $z = 0$ to $z = H$, then at the flame tip $m_t >> m_o$, $m_t u_a >> m_o u_o$, $m_t^2(w_c^3/2u_e) >> (m_o w_o)^2$ and tan A may be written as

$$\tan A = 2^{1/2}\left(\frac{u_a}{w_c}\right)\left(\frac{u_e}{w_c}\right)^{1/2} \tag{22}$$

Eqns 19 and 22 yield

$$\tan A = 2^{1/2}\eta^{1/2}\left(\frac{u_a}{w_c}\right)^{3/2} = 1.414\eta^{1/2}N_c^{-1/2} \tag{23}$$

where $(u_a/w_c)^3 = N_c^{-1}$. The alternative formulation for tan A using Eqn 20 in Eqn 22 leads to

$$\tan A = 2^{1/2}\alpha^{1/2}\left(\frac{u_a}{w_c}\right) = 1.414\alpha^{1/2}N_c^{-1/3} \tag{24}$$

Eqns 23 and 24 are suitable for evaluating entrainment constants η and α because the air/fuel ratio ϕ_f is missing from the two equations.

Flame height relationships

Anderson *et al.* (2006) noted that use of Froude number F_H in flame tilt angle models is problematic from the standpoint of prediction because flame height H is unknown. Moreover, one can infer from Albini (1981) that F_H is inversely proportional to convection number N_c. Two additional relationships for H in terms of fireline intensity I_B have been applied in various studies (Albini 1981; Anderson *et al.* 2006), but not in the context of combustion regimes delimited by $N_c = 10$. We explore these three flame height relationships using Eqn 14.

First, Eqns 2, 14, and 19 with $X_b = 1$ lead to

$$F_H = \frac{u_a^2}{gH} = \frac{2H_c\eta}{c_p T_a \phi_f N_c} = 100\left(\frac{\eta}{\phi_f}\right)N_c^{-1} \tag{25}$$

where η is obtained from a plot of Eqn 23. Second, a dimensional equation for H comes from combining Eqns 14 and 19 to yield

$$H = \frac{\phi_f I_B}{\rho_a H_c \eta u_a} = 0.0000556\left(\frac{\phi_f}{\eta}\right)\frac{I_B}{u_a} \tag{26}$$

where $\rho_a = 1.2$. Finally, Eqns 14, 18, and 20 combine to give

$$H = \frac{c_p T_a \phi_f w_c^2}{2gH_c\alpha} = \left(\frac{\phi_f^3 c_p T_a}{2g\rho_a^2\alpha^3 H_c^3}\right)^{1/3} I_B^{2/3} = 0.000147\left(\frac{\phi_f}{\alpha}\right)I_B^{2/3} \tag{27}$$

where α is evaluated using a plot of Eqn 24. We note that Eqn 27 is commonly used when $u_a = 0$; in such cases H, w_c, α and I_B should be written as H_o, w_{co}, α_o and I_{Bo}.

Comparison of flame characteristics data with model equations

The laboratory data are from fires in slash pine litter (*Pinus elliottii* Engelm.) and saw palmetto fronds (*Serenoa repens* (Bartram) Small) burned in the US Forest Service's Southern Forest Fire Laboratory (SFFL) wind tunnel in Macon, GA (Nelson and Adkins 1986). The February 1988 field measurements were made in 1-, 2- and 4-year roughs during experimental burns in southern rough fuels of northern Florida (Osceola National Forest) and longleaf pine (*Pinus palustris*-Mill.) litter–grass fuels of coastal South Carolina (Francis Marion National Forest). The field data, heretofore unpublished, are presented in Appendix A.

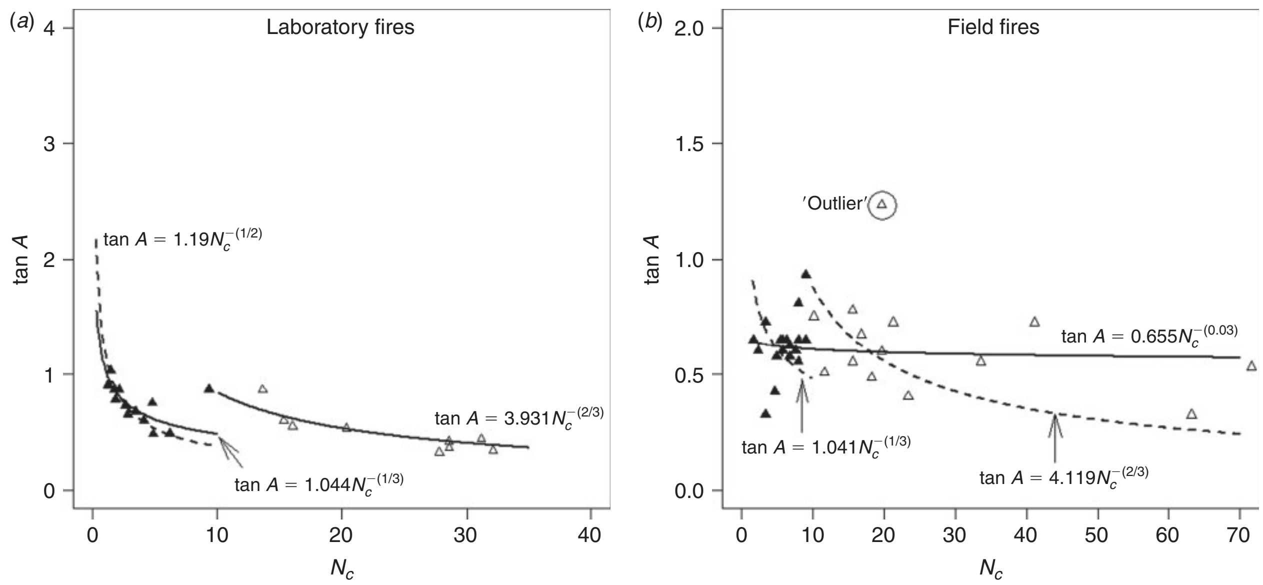

Fig. 2. Southern Forest Fire Laboratory (SFFL) laboratory (*a*) and field (*b*) data showing two behaviour regimes for $\tan A$ separating at a value of $N_c = 10$ for the laboratory data. For the field data, regressions (dashed lines) based on Eqn 24 for $N_c < 10$ and on Eqn 28 for $N_c > 10$ fit the data poorly. We select the regression for all N_c (solid line) as representative of $\tan A$ for the field data.

Fuel consumption in the field was estimated by weighing oven-dried pre- and post-burn fuels. In some cases, this led to overestimation of the available fuel load. Wind speeds were measured just behind the fireline with a hand-held digital wind meter at mid-flame height. Fire spread rate and flame characteristics were measured using the video methods of Nelson and Adkins (1986).

Theoretically, the data for tan A and H should pass through zero when the independent variable $X = 0$, so we set the intercept term to zero and fitted models of the form $Y = \gamma_1 X^\lambda$ where λ is an exponent determined analytically and γ_1 was estimated statistically by simple linear regression with unweighted least-squares for the model relationships in Eqns 23–27. Student's *t*-statistic tested significance of the parameter estimate. Overall quality of the regression models was evaluated using root mean squared error (RMSE) and mean absolute error (MAE). We used the Akaike Information Criterion (AIC_c), adjusted for small sample size (Burnham and Anderson 2004), to compare the different model formulations.

Because the commonly used coefficient of determination (R^2) can provide spurious information when the intercept term is set to zero (Eisenhauer 2003), we calculated R^2 as $R^2 = \sum \hat{Y}_i^2 / \sum Y_i^2$ to measure how much of the total variation of the dependent variable (also known as the uncorrected sum of squares) was described by our regression through the origin models. The models and their fit statistics are presented in Appendix B.

SFFL laboratory fires – flame tilt angle

The wind tunnel fires in beds of slash pine litter and slash litter under palmetto fronds were treated as coming from a single fuel type (Nelson and Adkins 1986). Initial fuel loads ranged from 0.5 to 1.1 kg m^{-2}, the dead fuel moisture content fraction from 0.09 to 0.13, and wind speed from 0.6 to 2.3 m s^{-1}. Palmetto frond fractional moisture content at the time of burning ranged from 0.9 to 1.25.

Fig. 2*a* is a plot of tan A according to Eqn 23 for all N_c. The data separate into two regimes at $N_c = 10$. The slope estimate of the line for $N_c < 10$ is 1.190, yielding $\eta = 0.71$. The data also are plotted according to Eqn 24 in Fig. 2*a*. The slope estimate of 1.044 for $N_c < 10$ implies $\alpha = 0.55$. These values of η and α are independent of ϕ_f, and are used in all subsequent evaluations of ϕ_f with the tan A and H equations. Thus we are assuming these η and α values also apply to the field fires, but only for $N_c < 10$.

Eqns 23 and 24 describe the data well for $N_c < 10$, but different behaviour is observed for $N_c > 10$. The theory appears valid only when an accretion mechanism is operative ($N_c < 10$). This is not surprising, as Eqns 12 and 19 were written to describe flames in moderately strong winds (Albini 1981).

An alternative theory is needed to describe tan A for $N_c > 10$. We assume that tan A for low winds (dynamic entrainment) is determined by a balance between transverse components of the drag force exerted on the flame by the impinging ambient air and the vertical buoyancy force resulting from combustion. Details of a model for tan A based on this approach are available in an Accessory publication (see http://www.publish.csiro.au/?act=view_file&file_id=WF10034_AC.pdf). It is shown that tan A for $N_c > 10$ is given by

$$\tan A = 3.85\eta^2 N_c^{-2/3} \qquad (28)$$

Fig. 2*a* also includes a plot of the regression of tan A on $N_c^{-2/3}$ for $N_c > 10$, $\tan A = 3.931 N_c^{-2/3}$, and suggests that Eqn 28 is a good description of the data. Though not significantly different from zero at the 0.05 level, the slope term was significantly different at the 0.077 level; thus $\eta = (3.93/3.85)^{1/2} = 1.01$. The $\eta = 1$ estimate for $N_c > 10$ implies that fires in light winds entrain a larger fraction of the impinging air (the total amount

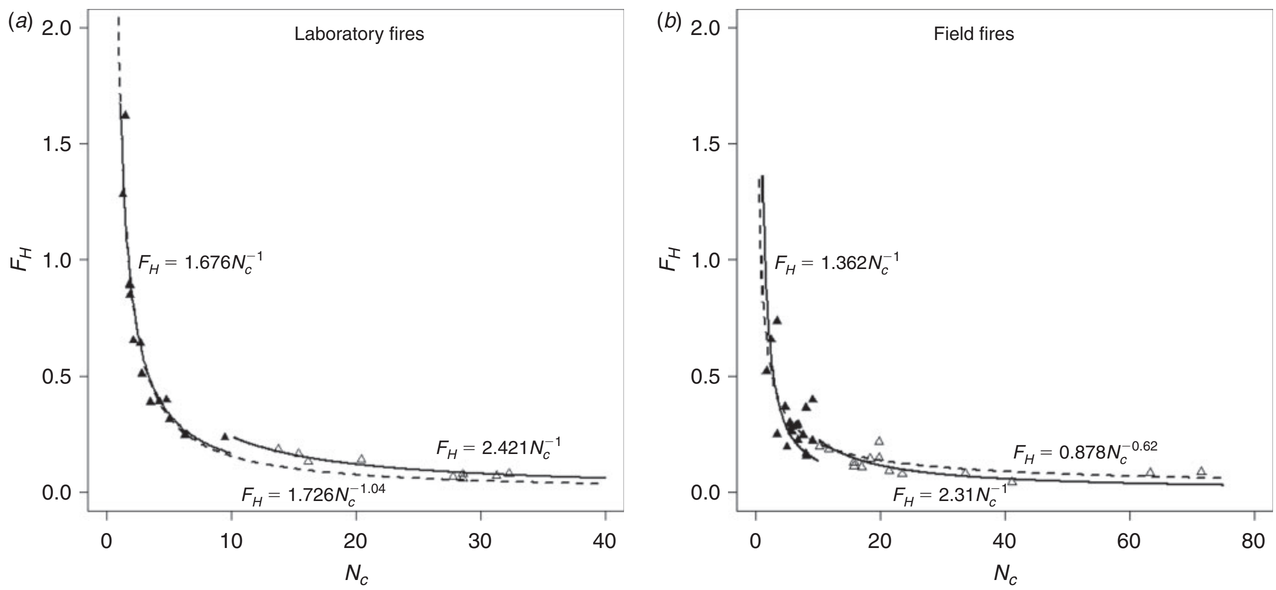

Fig. 3. Southern Forest Fire Laboratory (SFFL) laboratory (*a*) and field (*b*) data showing that the relationship between F_H and N_c is similar for both datasets and that regression suggests a slight difference at approximately $N_c = 10$. Solid lines denote fitted equations based on the N_c criterion; dashed lines illustrate fitted regressions using all N_c data.

is relatively small) than fires in stronger winds ($N_c < 10$) for which the value $\eta = 0.71$ was estimated earlier.

It was not possible to determine α by using Eqn 20 to derive an equation similar to Eqn 28 because the result would imply $\tan A = \text{constant}$. Fig. 2*a* shows that $\tan A$ for $N_c > 10$ is not constant, but described well by Eqn 28. Thus, only Eqn 19 describes the entrainment velocity and flame tilt angle for $N_c > 10$. This result may be due to suppression of vertical flow in the SFFL tunnel. We believe a result approximating $\tan A = \text{constant}$ is representative of fires in large wind tunnels.

SFFL field fires – flame tilt angle

For the palmetto–gallberry fuels, flame heights ranged from 0.4 m in 1-year roughs to 5 m in the 4-year roughs; in the litter–grass fuels, flame heights exhibited intermediate values. Fractional moisture content of the dead grass was 0.18; the L and F layers ranged from 0.2 to 0.5, and the live palmetto fronds and gallberry leaves from 1 to 1.4.

Eqns 23–24 describe the $\tan A$ laboratory data for $N_c < 10$, but not the corresponding field data (Fig. 2*b*); a regression according to Eqn 24 leads to $\tan A = 1.041 N_c^{-1/3}$, an extremely poor fit (a brief discussion of flame tilt angle in the wind tunnel and field is available in an Accessory publication, see www.publish.csiro.au/?act=view_file&file_id=WF10034_AC.pdf). The linear increase in $\tan A$ is physically questionable and disagrees with the numerical modelling results of Nmira *et al.* (2010) and the experimental data of Fendell *et al.* (1990) discussed by Alexander (1998); these investigators show that $\tan A$ should be proportional to a reciprocal power of N_c smaller than unity. Thus we consider the four outermost data points for $N_c < 10$ as outliers due to errors in measurement of $\tan A$ and available fuel load W_a; ignoring these points suggests $\tan A = \text{constant}$.

To study Eqn 28 for $N_c > 10$, we plotted $\tan A$ *v.* N_c in Fig. 2*b*. An outlying point initially was neglected in both the plot and regression; the result, $\tan A = 4.119 N_c^{-2/3}$, yields $\eta = (4.12/3.85)^{1/2} = 1.03$ and supports the earlier result for the laboratory data, $\eta = 1$ when $N_c > 10$. Including the outlier in the regression $\tan A = 4.458 N_c^{-2/3}$ produces a slope estimate not significantly different from 4.119; however, the fit statistics are less desirable for $N_c > 20$.

Although Eqn 28 is a possible descriptor of $\tan A$ for $N_c > 10$ and useful for estimating η for the field fires, inspection of all data in Fig. 2*b* suggests that $\tan A$ is best described as constant. For example, we consider 26 of the 32 data points in the figure to approximate the horizontal line $\tan A = 0.65$. We have regressed all data as coming from a single population of $\tan A$ values and compared the results with statistics obtained from regressing the data according to $N_c < 10$ and $N_c > 10$. The statistical fit based on all data (outlier removed) is superior to the fits obtained when the data are separated into two groups (Appendix B). Thus the single-regression equation, $\tan A = 0.655 N_c^{-0.03}$, indicates that flame tilt angle for the field data is given by $\tan A = 0.655$ – a behaviour not seen in the laboratory fires.

The result $\tan A = \text{constant}$ for all N_c can be derived from the idea that flame tilt is determined by a balance involving rates at which work is done by rising parcels of flame and parcels of moving air. An equation based on this approach is available in an Accessory publication (see http://www.publish.csiro.au/?act=view_file&file_id=WF10034_AC.pdf). Setting $\tan A$ in this equation to 0.655,

$$\tan A = \frac{C_D \rho_a \alpha^3}{\rho_c} = 3.85\alpha^3 = 0.655 \qquad (29)$$

and $\alpha = 0.55$, in agreement with the laboratory fire estimate. This result supports our assumption that the laboratory fire

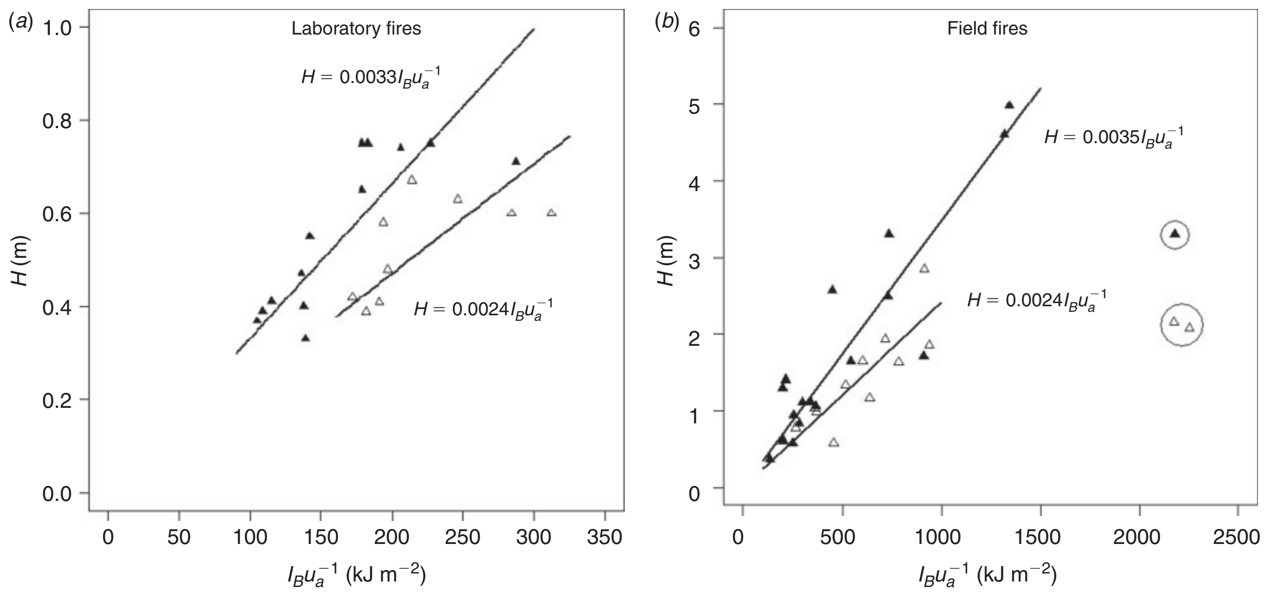

Fig. 4. Southern Forest Fire Laboratory (SFFL) laboratory (*a*) and field (*b*) data indicating that the H *v*. $I_B u_a^{-1}$ relationship is linear; dark triangles denote $N_c < 10$, open triangles $N_c > 10$. Both the laboratory and field data are scattered, but divided into separate regions according to N_c. Three outliers in the field data are omitted from the regressions.

results, $\eta = 0.71$ and $\alpha = 0.55$ for $N_c < 10$ and $\eta = 1$ for $N_c > 10$, can be used to calculate ϕ_f for the field fires. This constant-angle regime of burning is referred to as *kinetic entrainment.*

SFFL laboratory and field fires – flame height

The height H of wind-blown flames is described by Eqns 25–27. For the laboratory data, F_H and N_c are plotted in Fig. 3*a* using Eqn 25; the estimated slope is 1.676 for $N_c < 10$. Thus for $\eta = 0.71$, $\phi_f = 42.4$. For $N_c > 10$, the slope is 2.421, so with $\eta = 1$, $\phi_f = 41.3$. A regression using all data yielded $F_H = 1.726 N_c^{-1.04}$, which was significant (Appendix B).

Fig. 3*b* for the field data shows plots of F_H *v*. N_c according to Eqn 25. For $N_c < 10$, $F_H = 1.362 N_c^{-1}$ and the slope estimate with $\eta = 0.71$ yields $\phi_f = 52.2$. For $N_c > 10$, $F_H = 2.310 N_c^{-1}$, giving $\phi_f = 43$ for $\eta = 1$. If the $N_c = 10$ criterion is not applied and all data are considered, a model in which both the slope and exponent were estimated from the data, $F_H = 0.878 N_c^{-0.62}$, is a better fit than a model that assumed the N_c^{-1} formulation, $F_H = 1.397 N_c^{-1}$ (not shown in Fig. 3*b*).

For $N_c = 10$ in Fig. 3, $F_H \approx 0.25$ for the laboratory and field fires. Pagni and Peterson (1973) and Morvan and Dupuy (2004) state that when flame-length Froude number $F_L < 0.25$, fire spread in pine needle beds is radiation (buoyancy)-controlled and flame tilt is close to vertical; when $F_L > 1$, the spread rate is controlled by a combination of radiation and convection. Neglecting the small difference between F_L and F_H for our fires, we interpret the intermediate region $0.25 < F_H < 1$ as one in which radiative preheating decreases as $F_H \rightarrow 1$ while the convective contribution due to wind increases. For $F_H > 1$, fire spread becomes increasingly wind-driven. Because $F_H > 1$ for only two of our laboratory fires, this regime requires further study.

The second relationship for flame height is Eqn 26, which relates H to $I_B u_a^{-1}$. The data in Fig. 4*a* show two burning regimes. For $N_c < 10$, $H = 0.0033 I_B u_a^{-1}$; thus for $\eta = 0.71$, Eqn 26 yields $\phi_f = 42.4$ – in agreement with the corresponding laboratory value. For $N_c > 10$, $H = 0.0024 I_B u_a^{-1}$ and $\phi_f = 42.4$ if $\eta = 1$.

The field data in Fig. 4*b* show three outliers (circled), and preliminary regressions for all data points resulted in poor fits. These outliers were explained by exploratory plots that showed that W_a for the three points was overestimated by a factor of 2. Reduction of fireline intensity I_B by this factor places the data points close to their respective regression lines. When the regressions were repeated with outliers omitted, the equation for $N_c < 10$, $H = 0.0035 I_B u_a^{-1}$, resulted in $\phi_f = 44.3$; for $N_c > 10$, the equation $H = 0.0024 I_B u_a^{-1}$ gave $\phi_f = 43.3$. With outliers removed, ϕ_f for the laboratory and field fires agreed closely.

The third equation, Eqn 27, describes H in terms of $I_B^{2/3}$. The laboratory data plotted in Fig. 5*a* are scattered, with a tendency for $N_c > 10$ data to be associated with lower I_B. We accepted Eqn 27 as a descriptor of the data in Fig. 5*a* for two reasons. First, the fitted regression for all laboratory fire data in Fig. 5*a*, $H = 0.0142 I_B^{2/3}$, was not statistically different from the corresponding regression for all field data (Fig. 5*b*). Second, even though two points from each N_c regime overlap into the other regime, R^2 values for both N_c regimes in Fig. 5*a* exceed 0.95. For $N_c < 10$, $H = 0.0132 I_B^{2/3}$ and $\phi_f = 49.4$ when $\eta = 0.71$. For $N_c > 10$, $H = 0.0173 I_B^{2/3}$, which gives $\phi_f = 64.7$ if $\eta = 1$.

Plots of the field data according to Eqn 27 are shown in Fig. 5*b*. Separate regressions for $N_c < 10$ and $N_c > 10$ (not presented) produced slope estimates of 0.0138 and 0.0137 respectively, so there was no suggestion of two burning regimes dependent on N_c. A single line with a slope of 0.0137 for all data did not describe the bulk of the data; thus, the most outlying point was not included in a new regression. The slope estimate of

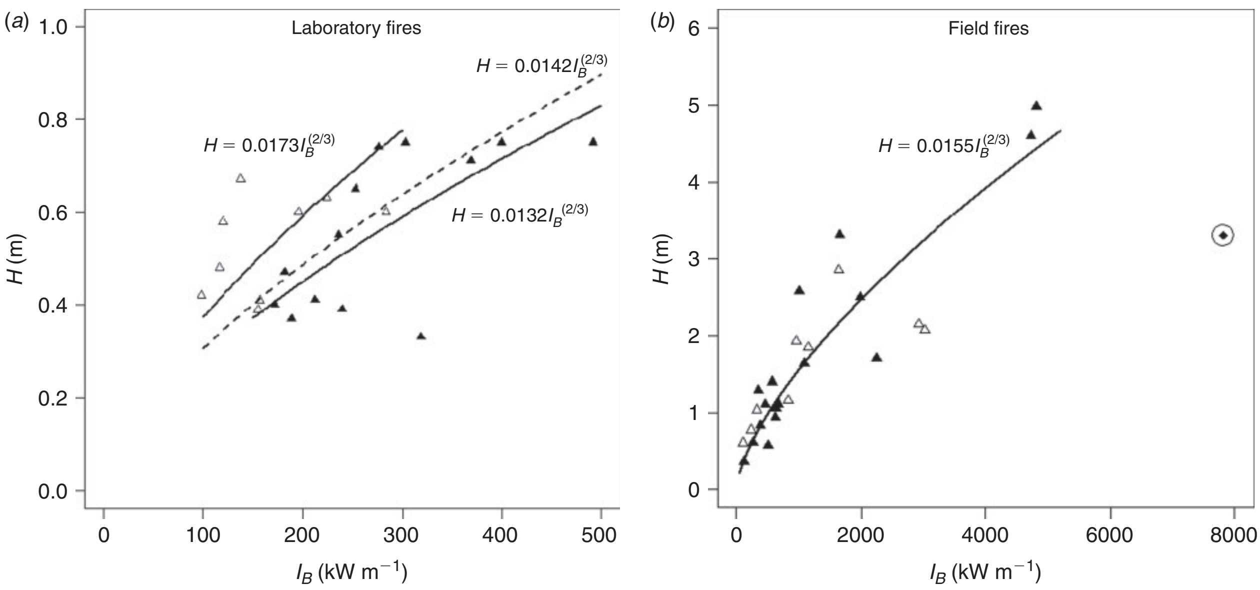

Fig. 5. Southern Forest Fire Laboratory (SFFL) laboratory (*a*) and field (*b*) data suggesting similar trends for H *v.* I_B; dark triangles denote $N_c < 10$, open triangles $N_c > 10$. Solid lines are regression results; dashed line for the laboratory data denotes a regression for all N_c. Ranges of H and I_B in the laboratory data constitute only a small fraction of the corresponding ranges in the field data. Circled data point is an outlier.

Table 1. Individual and averaged entrainment parameters and air/fuel ratios for Southern Forest Fire Laboratory (SFFL) laboratory and field fires

Flame characteristics	Model equations	Entrainment constants				Air/fuel ratios			
		η		α		ϕ_f		ϕ_{cz}	
		$N_c < 10$	$N_c > 10$	$N_c < 10$	$N_c > 10$	$N_c < 10$	$N_c > 10$	$N_c < 10$	$N_c > 10$
SFFL laboratory									
tan A	23	0.71	–	0.55	–	–	–	–	–
tan A	28	–	1.01	–	–	–	–	–	–
F_H	25	–	–	–	–	42.4	41.3	15.7	15.2
H	26	–	–	–	–	42.4	42.4	15.7	15.7
H	27	–	–	–	–	49.4	64.7	18.5	24.6
Laboratory average		0.71	1.01	0.55	–	44.7	49.5	16.6	18.5
SFFL field									
tan A	28	–	1.03	–	–	–	–	–	–
tan A	29	–	–	0.55	0.55	–	–	–	–
F_H	25	–	–	–	–	52.2	43.3	19.6	16.0
H	26	–	–	–	–	44.3	43.3	16.4	16.0
H	27	–	–	–	–	58.0	58.0	21.9	21.9
Field average		–	1.03	0.55	0.55	51.5	48.2	19.3	18.0
Overall average		0.71	1.02	0.55	0.55	48.1	48.9	18.0	18.3

the resulting regression, $H = 0.0155I_B^{2/3}$, implies $\phi_f = 58$ if $\alpha = 0.55$. This equation has fit statistics similar to the corresponding regression for all laboratory data, $H = 0.0142I_B^{2/3}$. Apparently, use of Eqn 20 for u_e masks any dependence of H on u_a or N_c under field conditions.

Summary of results

Numerical models describing wildland fire (Porterie *et al.* 2000; Morvan 2007; Nmira *et al.* 2010) identify a low-wind combustion regime where buoyant forces exceed ambient wind inertial forces, and a moderate-to-high wind regime in which the dominant force is exerted by the wind. To a large extent, these results are supported by findings of the present study. Experimental data for the SFFL laboratory and field head fires showed that the criterion $N_c = 10$ often indicated transition from dynamic entrainment ($N_c > 10$) to accretive entrainment ($N_c < 10$) as wind speed increased. These two burning regimes are likely to appear in analyses of tan A and H involving wind speed u_a – i.e. use of Eqn 19 for entrainment velocity u_e. Alternately, when Eqn 20 for u_e was used, tan A in the field data was essentially constant. The presence of fireline intensity I_B in the analysis of flame height H in the field fires seemed to incorporate the effects of u_a on H automatically; thus for all values of N_c, the fires burned in a single regime. This result differed from laboratory fire data for H *v.* I_B (Fig. 5*a*), which separated according to N_c. The difference may be due to experimental design (three fuel groups with constant W_a within groups) and confined buoyant convection in the SFFL wind tunnel.

Entrainment parameters and flame zone air/fuel mass ratios are summarised in Table 1. Accretive and dynamic regimes of entrainment are indicated by $N_c < 10$ and $N_c > 10$ respectively. The combustion zone air/fuel ratio ϕ_{cz} is calculated from Eqns 14 as:

$$\phi_{cz} = 0.4\phi_f - \left(\frac{1}{X_b}\right) = 0.4\phi_f - 1.3 \qquad (30)$$

with volatile burn fraction X_b taken as 0.75. Table 1 gives an overall air/fuel ratio, $\phi_{cz} + \phi_f$, equal to 67 kg kg^{-1} – a value within the range 60–80 kg kg^{-1} (Thomas *et al.* 1965). The earlier theoretical estimates, $\phi_f = 50$ and $\phi_{cz} = 20$ kg kg^{-1}, compare favourably with the semi-empirical values in Table 1.

The laboratory fires duplicated the field fires with two exceptions. First, for $N_c < 10$, tan A for the laboratory fires was proportional to $N_c^{-1/2}$ or $N_c^{-1/3}$, whereas tan A for the field fires was independent of N_c. The Albini (1981) model for flame tilt angle, tan $A = u/w$, was descriptive of only the $N_c < 10$ data from the SFFL wind tunnel, requiring two additional models for describing tilt angle: (1) Eqn 28 for low-wind-speed fires in the tunnel, and (2) Eqn 29 for all data from the field experiments. The second exception was that the laboratory data for H tended to separate according to the $N_c = 10$ criterion, whereas the field data exhibited a similar relationship, but without the N_c separation. These differences among tan A, H, I_B and N_c seem related to experimental design and the fire environments, rather than to fuel or wind-speed differences. Froude number F_H was proportional to N_c^{-1} for both burning regimes; H was proportional to $I_B u_a^{-1}$ and to $I_B^{2/3}$ for both the laboratory and field fires.

Conclusions

The objectives of this study were to: (1) develop criteria to determine whether differences in observed flame characteristics can be related to differences in air entrainment mechanisms; (2) derive equations for relating flame height and tilt angle to commonly used fire behaviour variables and entrainment parameters; and (3) develop estimates of entrainment parameters by using the model equations and regression methods to generate statistical fits of the laboratory and field data. Specific conclusions drawn from the present work are:

1. Two burning regimes are found in laboratory wind-tunnel fires in slash pine litter beds; the same regimes are present in field fires in the palmetto–gallberry and longleaf pine litter–grass fuel types. Transition from a low wind speed to a higher wind speed regime is indicated by $N_c = 10$.
2. Equations for flame tilt angle and flame height generally describe the experimental tilt angles and heights well. For the field fires, tan A is constant rather than a power function of reciprocal N_c. Kinetic energy fluxes in the ambient air and flame describe the constant tilt angle regime. Laboratory data for the H *v.* $I_B^{2/3}$ relationship separate according to the $N_c = 10$ criterion, but the field data for H do not separate.
3. Air enters head fire flames by: (i) dynamic entrainment ($N_c > 10$) in which the entrainment velocity approximates the mid-flame wind speed, or (ii) accretion ($N_c < 10$) in which air is blown into the flame either at a velocity equal to 71% of the mid-flame wind speed, u_a, or at a velocity equal to 55% of the characteristic vertical flame velocity, w_c.
4. The mean velocity of entrainment, u_e, is proportional to either ambient wind speed u_a with proportionality constant η, or to the characteristic buoyant velocity w_c with proportionality constant α. For moderate winds ($N_c < 10$), these semi-empirical constants from the laboratory data are $\eta = 0.71$ and $\alpha = 0.55$ (assumed equal for both laboratory and field fires). For low winds ($N_c > 10$), $\eta = 1.02$; no value is available for α.
5. Theoretical flame-zone air/fuel ratio ϕ_f is 50 kg kg^{-1}; combustion-zone air/fuel ratio ϕ_{cz} is 20 kg kg^{-1}. Corresponding experimental ratios (averaged for laboratory and field burns over all N_c) are 48.5 and 18.2. Thus the theoretical overall air/fuel ratio of 70 compares favourably with the semi-empirical ratio of 67.
6. Field fires in the southern rough and longleaf litter–grass fuel types can be simulated well with laboratory wind-tunnel fires insofar as estimates of the air/fuel mass ratio and flame height are concerned, but tangent of the flame tilt angle is sensitive to environmental conditions.

Symbols used in mathematical models

Roman symbols

A, flame tilt angle from vertical (degrees of angle)
A_f, flow area of flame (m^2)
A_p, projected flame area (m^2)
b_F, fireline buoyancy flux (m^3 m^{-3})
b_R, ocean plume buoyancy flux (m^3 m^{-3})
C_D, flame drag coefficient
cos A, cosine of angle A
c_p, constant-pressure specific heat of burned and unburned volatiles, flame fluid and air (kJ kg^{-1} K^{-1})
D, horizontal width of flame at z (m)
D_o, flame depth at $z = 0$ (m)
F_B, flame buoyant force (kg m s^{-2})
F_D, horizontal drag force on flame (kg m s^{-2})
F_H, flame height Froude number
F_F, fire Froude number
F_L, flame length Froude number
F_R, effluent plume Froude number
f, fraction of original moisture remaining after preheating
g, acceleration of gravity (m s^{-2})
H, flame height (m)
H_c, convective low heat of combustion (kJ kg^{-1})
I_B, overall fireline intensity (kW m^{-1})
I_{Bcz}, combustion zone contribution to I_B (kW m^{-1})
L, unit length of fireline (m)
M, fractional moisture content
M_e, mass of an entrained air parcel (kg)
m, vertical mass flow rate at z (kg m^{-1} s^{-1})
m_o, vertical mass flow rate at $z = 0$ (kg m^{-1} s^{-1})

m_t, vertical mass flow rate at $z = H$ (kg m^{-1} s^{-1})
N_c, convection number
N_v, stoichiometric air/fuel mass ratio of volatiles (kg kg^{-1})
Δp, pressure drop in flame (kg m^{-1} s^{-2})
q, effluent volumetric discharge rate per unit length of diffuser (m^2 s^{-1})
R, rate of fire spread (m s^{-1})
sec A, secant of angle A
T, mean flame temperature at z (K)
T_a, ambient air temperature (K)
T_o, mean flame temperature at $z = 0$ (K)
T_t, mean flame temperature at $z = H$ (K)
t, time (s)
u, horizontal component of flame velocity at z (m s^{-1})
u_a, mid-flame ambient wind speed (m s^{-1})
u_c, horizontal ocean current speed (m s^{-1})
u_e, mean entrainment velocity (m s^{-1})
u_o, mean value of u at z = 0 (m s^{-1})
v, mean axial flame velocity at z (m s^{-1})
V, volume of heated air parcel of mass M_e (m^3)
V_o, volume of ambient air parcel of mass M_e (m^3)
W, mean work done by parcels of air or flame (kg m^2 s^{-2})
W_a, available fuel loading (kg m^{-2})
w, vertical component of flame velocity at z (m s^{-1})
w_c, characteristic buoyant velocity (m s^{-1})
w_{co}, w_c for zero-wind fires (m s^{-1})
w_o, mean value of w at $z = 0$ (m s^{-1})
X_b, fraction of volatiles produced that burns
$Y_i, \hat{Y}_{i,}$ observed and predicted value of dependent variable respectively
Z, mass of unreacted air in the combustion zone per mass of original fuel
z, vertical distance above fuel bed surface (m)

Greek symbols

α, entrainment constant
α_o, entrainment constant when $u_a = 0$
$\gamma_1, \hat{\gamma}_1$, analytically derived and statistically estimated values of power function coefficient
λ, analytically derived exponent
$\Delta\rho$, density difference between diffuser effluent and ambient water (kg m^{-3})
ε, combustion efficiency
η, entrainment constant
ρ, flame mass density at z (kg m^{-3})
ρ_a, ambient air mass density (kg m^{-3})
ρ_c, flame mean mass density (kg m^{-3})
ρ_e, diffuser effluent mass density (kg m^{-3})
ρ_o, flame mass density at $T = T_o$ (kg m^{-3})
ϕ_{cz}, combustion zone mean air/fuel mass ratio
ϕ_f, free flame mean air/fuel ratio

Acknowledgements

We thank Dale Wade, Ted Ach, Wayne Adkins and Hilliard Gibbs, all formerly of the Southern Forest Fire Laboratory, Macon, GA, for their aid in burn plot preparation and collection of fire behaviour data during the 1988 controlled burns in FL and SC. We also thank anonymous reviewers for their helpful suggestions.

References

Albini FA (1980) Thermochemical properties of flame gases from fine wildland fuels. USDA Forest Service, Intermountain Forest and Range Experiment Station Research Paper INT-243. (Ogden, UT)

Albini FA (1981) A model for the wind-blown flame from a line fire. *Combustion and Flame* **43**, 155–174. doi:10.1016/0010-2180(81)90014-6

Albini FA, Brown JK, Reinhardt ED, Ottmar RD (1995) Calibration of a large fuel burnout model. *International Journal of Wildland Fire* **5**, 173–192. doi:10.1071/WF9950173

Alexander ME (1998) Crown fire thresholds in exotic pine plantations of Australasia. PhD thesis, Australian National University, Canberra.

Anderson W, Pastor E, Butler B, Catchpole E, Dupuy JL, Fernandes P, Guijarro M, Mendes-Lopes JM, Ventura J (2006) Evaluating models to estimate flame characteristics for free-burning fires using laboratory and field data. In 'Proceedings, V International Conference on Forest Fire Research', 27–30 November 2006, Figueira da Foz, Portugal. (Ed. DX Viegas) (CD-ROM) (Elsevier BV: Amsterdam)

Anderson W, Catchpole E, Butler B (2010) Measuring and modeling convective heat transfer in front of a spreading fire. *International Journal of Wildland Fire* **19**, 1–15.

Beer T (1991) The interaction of wind and fire. *Boundary-Layer Meteorology* **54**, 287–308. doi:10.1007/BF00183958

Beer T (1993) The speed of a fire front and its dependence on wind speed. *International Journal of Wildland Fire* **3**, 193–202. doi:10.1071/WF9930193

Burnham KP, Anderson DR (2004) Multimodel inference: understanding AIC and BIC in model selection. *Sociological Methods & Research* **33**, 261–304. doi:10.1177/0049124104268644

Burrows ND (1994) Experimental development of a fire management model for jarrah (*Eucalyptus marginata* Donn ex Sm.) forest. PhD thesis, Australian National University, Canberra.

Byram GM (1959) Forest fire behavior. In 'Forest Fire: Control and Use'. (Ed. KP Davis) pp. 61–89. (McGraw-Hill: New York)

Byram GM, Nelson RM, Jr (1974) Buoyancy characteristics of a fire heat source. *Fire Technology* **10**, 68–79. doi:10.1007/BF02590513

Cruz ME, Alexander ME (2010) Assessing crown fire potential in coniferous forests of western North America: a critique of current approaches and recent simulation studies. *International Journal of Wildland Fire* **19**, 377–398. doi:10.1071/WF08132

Eisenhauer JG (2003) Regression through the origin. *Teaching Statistics* **25**, 76–80. doi:10.1111/1467-9639.00136

Fang JB (1969) An investigation of the effect of controlled wind on the rate of fire spread. PhD thesis, University of New Brunswick, Fredericton, NB.

Fendell FE, Carrier GF, Wolff MF (1990) Wind-aided fire spread across arrays of discrete fuel elements. US Department of Defense, Defense Nuclear Agency, Technical Report DNA-TR-89–193. (Alexandria, VA)

Fernandes PM, Botelho HS, Loureiro C (2002) Models for the sustained ignition and behavior of low-to-moderately intense fires in maritime pine stands. In 'IV International Conference on Forest Fire Research/2002 Wildland Fire Safety Summit', 18–20 November 2002, Luso, Portugal. (Ed. DX Viegas) (CD-ROM) (Millpress: Rotterdam)

Fleeter RD, Fendell FE, Cohen LM, Gat N, Witte AB (1984) Laboratory facility for wind-aided fire spread along a fuel matrix. *Combustion and Flame* **57**, 289–311. doi:10.1016/0010-2180(84)90049-X

Linn RR, Cunningham P (2005) Numerical simulations of grass fires using a coupled atmosphere–fire model: basic fire behavior and dependence on wind speed. *Journal of Geophysical Research* **110**, D13107. doi:10.1029/2004JD005597

Lozano J, Tachajapong W, Weise DR, Mahalingam S, Princevac M (2010) Fluid dynamic structures in a fire environment observed in laboratory-scale experiments. *Combustion Science and Technology* **182**, 858–878. doi:10.1080/00102200903401241

Mendes-Lopes JMC, Ventura JMP, Amaral JMP (1998) Rate of spread and flame characteristics in a bed of pine needles. In 'Proceedings: Third International Conference on Forest Fire Research and Fourteenth Conference on Fire and Forest Meteorology', 16–20 November 1998, Luso, Portugal. (Ed. DX Viegas) pp. 497–511. (University of Coimbra: Portugal)

Mendes-Lopes JMC, Ventura JMP, Amaral JMP (2003) Flame characteristics, temperature–time curves, and rate of spread in fires propagating in a bed of *Pinus pinaster* needles. *International Journal of Wildland Fire* **12**, 67–84. doi:10.1071/WF02063

Morvan D (2007) A numerical study of flame geometry and potential for crown fire initiation for a wildfire propagating through shrub fuel. *International Journal of Wildland Fire* **16**, 511–518. doi:10.1071/WF06010

Morvan D, Dupuy JL (2004) Modeling the propagation of a wildfire through a Mediterranean shrub using a multiphase formulation. *Combustion and Flame* **138**, 199–210. doi:10.1016/J.COMBUSTFLAME.2004.05.001

Nelson RM, Jr (1980) Flame characteristics for fires in southern fuels. USDA Forest Service, Southeastern Forest Experiment Station, Research Paper SE-205. (Asheville, NC)

Nelson RM, Jr (1993) Byram's derivation of the energy criterion for forest and wildland fires. *International Journal of Wildland Fire* **3**, 131–138. doi:10.1071/WF9930131

Nelson RM, Jr (2003) Power of the fire – a thermodynamic analysis. *International Journal of Wildland Fire* **12**, 51–65. doi:10.1071/WF02032

Nelson RM, Jr, Adkins CW (1986) Flame characteristics of wind-driven surface fires. *Canadian Journal of Forest Research* **16**, 1293–1300. doi:10.1139/X86-229

Nelson RM, Jr, Adkins CW (1988) A dimensionless correlation for the spread of wind-driven fires. *Canadian Journal of Forest Research* **18**, 391–397. doi:10.1139/X88-058

Nmira F, Consalvi JL, Boulet P, Porterie B (2010) Numerical study of wind effects on the characteristics of flames from non-propagating vegetation fires. *Fire Safety Journal* **45**, 129–141. doi:10.1016/J.FIRESAF.2009.12.004

Pagni PJ, Peterson TG (1973) Flame spread through porous fuels. In 'Proceedings of the Fourteenth Symposium (International) on Combustion', 20–25 August 1972, University Park, PA. pp. 1099–1107. (The Combustion Institute: Pittsburgh, PA)

Porterie B, Morvan D, Loraud JC, Larini M (2000) Firespread through fuel beds: modeling of wind-aided fires and induced hydrodynamics. *Physics of Fluids* **12**, 1762–1782. doi:10.1063/1.870426

Roberts PJW (1979) Line plume and ocean outfall dispersion. *Journal of the Hydraulics Division – Proceedings of the American Society of Civil Engineers* **105**(HY4), 313–331

Roberts PJW, Snyder WH, Baumgartner DJ (1989) Ocean outfalls. III. Effect of diffuser design on submerged wastefield. *Journal of Hydraulic Engineering* **115**, 49–70. doi:10.1061/(ASCE)0733-9429(1989)115:1(49)

Sun L, Zhou X, Mahalingam S, Weise DR (2006) Comparison of burning characteristics of live and dead chaparral fuels. *Combustion and Flame* **144**, 349–359. doi:10.1016/J.COMBUSTFLAME.2005.08.008

Tachajapong W, Lozano J, Mahalingam S, Weise DR (2008) An investigation of crown fuel bulk density effects on the dynamics of crown fire initiation. *Combustion Science and Technology* **180**, 593–615. doi:10.1080/00102200701838800

Taylor GI (1961) Fire under the influence of natural convection. In 'The Use of Models in Fire Research'. (Ed. WG Berl) National Academy of Science, National Research Council Publication 786, pp. 10–32. (Washington, DC)

Thomas PH (1963) The size of flames from natural fires. In 'Proceedings of the Ninth Symposium (International) on Combustion', 27 August–1 September 1962, Ithaca, NY. pp. 844–859. (The Combustion Institute: Pittsburgh, PA)

Thomas PH (1964) The effect of wind on plumes from a line heat source. Department of Scientific and Industrial Research, Fire Research Station, Fire Research Note 572. (Boreham Wood, UK)

Thomas PH (1967) Some aspects of the growth and spread of fires in the open. *Forestry* **40**, 139–164. doi:10.1093/FORESTRY/40.2.139

Thomas PH, Pickard RW, Wraight HGH (1963) On the size and orientation of buoyant diffusion flames and the effect of wind. Department of Scientific and Industrial Research, Fire Research Station, Fire Research Note 516. (Boreham Wood, UK)

Thomas PH, Baldwin R, Heselden AJM (1965) Buoyant diffusion flames: some measurements of air entrainment, heat transfer, and flame merging. In 'Proceedings of the Tenth Symposium (International) on Combustion', 14–20 July 1968, Poitiers, France. pp. 983–996. (The Combustion Institute: Pittsburgh, PA)

Van Wagner CE (1968) Fire behavior mechanisms in a red pine plantation: field and laboratory evidence. Canadian Department of Forestry and Rural Development, Forestry Branch Publication 1229m. (Ottawa, ON)

Weise DR, Biging GS (1996) Effects of wind velocity and slope on flame properties. *Canadian Journal of Forest Research* **26**, 1849–1858. doi:10.1139/X26-210

Zhou X, Mahalingham S, Weise D (2005) Modeling of marginal burning state of fire spread in live chaparral shrub fuel bed. *Combustion and Flame* **143**, 183–198. doi:10.1016/J.COMBUSTFLAME.2005.05.013

Appendix A. Southern Forest Fire Laboratory (SFFL) 1988 field data

Fire number	R (m s^{-1})	W_a (kg m^{-2})	u_a (m s^{-1})	D_o (m)	H (m)	I_B (kW m^{-1})	N_c	tan A
OS1A1[A]	0.063	0.534	2.03	0.68	0.57	505	3.32	0.727
OS1A2	0.076	0.552	1.74	0.53	1.06	634	6.72	0.577
OS1B1	0.043	0.370	0.91	0.56	0.78	239	16.86	0.675
OS1C1	0.073	0.527	2.68	0.68	1.40	577	1.63	0.649
OS1D1	0.063	0.279	1.31	0.52	0.61	264	6.35	0.649
OS1D2	0.092	0.605	1.31	0.91	1.16	834	19.74	0.601
OS1E1	0.065	0.397	1.37	0.66	0.83	387	8.00	0.810
OS1E2	0.019	0.366	0.51	0.40	0.61	102	41.00	0.727
OS1F1	0.036	0.226	0.90	0.41	0.37	122	9.04	0.933
OS1F2	0.053	0.643	1.12	0.56	0.58	511	19.74	1.235
OS2A1	0.043	0.972	2.46	0.68	0.94	627	2.28	0.601
OS2B1	0.122	1.100	2.70	1.35	2.50	1980	5.40	0.649
OS2C1	0.125	0.536	2.24	1.81	2.58	1004	4.87	0.577
OS2D1	0.100	0.765	1.22	1.13	1.85	1147	33.57	0.554
OS2D2	0.046	0.983	2.00	0.57	1.11	678	4.63	0.424
OS2E1	0.085	0.755	1.34	0.92	1.93	964	21.43	0.727
OS2E2	0.144	1.350	1.34	1.24	2.15	2915	64.00	0.325
OS2F1	0.048	0.444	0.90	0.75	1.04	323	23.32	0.404
OS4B1	0.226	0.483	1.79	1.39	2.85	1638	15.63	0.554
OS4B2	0.120	0.600	2.00	1.23	1.64	1084	7.54	0.601
OS4C1	0.259	2.010	3.59	1.45	3.30	7824	9.04	0.649
OS4C2	0.136	1.480	1.34	1.10	2.07	3016	72.34	0.532
OS4D1	0.301	1.050	3.59	2.66	4.60	4728	5.69	0.649
OS4D2	0.341	0.945	3.59	3.55	4.97	4818	5.69	0.601
FM1A2[B]	0.102	0.272	1.12	0.62	0.98	416	15.63	0.781
FM1D1	0.087	0.620	1.57	0.59	1.33	809	11.74	0.510
FM2A1	0.154	0.466	1.79	0.95	1.64	1076	10.27	0.754
FM2A2	0.168	0.889	2.46	1.02	1.70	2240	8.00	0.649
FM2C1	0.054	0.575	1.57	0.61	1.11	466	6.72	0.625
FM2D1	0.052	0.459	1.79	0.67	1.29	355	3.32	0.325
FM4A1	0.298	0.370	2.24	1.73	3.30	1654	8.00	0.554
FM4D1	0.138	0.578	1.52	0.74	1.63	1196	18.22	0.488

[A]OS1A1 denotes a fire in the Osceola National Forest, 1-year rough, plot A1.
[B]FM1A2 denotes a fire in the Francis Marion National Forest, 1-year rough, plot A2.

Appendix B. Regression equations and statistical fits of the model equations to experimental data

t-test results show if a parameter estimate = 0. Y indicates that the estimate is significantly different from zero (rejected null hypothesis). N indicates that the null hypothesis was not rejected. Probability value of *t*-value ≤ 0.05 defined as significant. Fit statistics are:

$$R^2 = \frac{\sum \hat{Y}_i^2}{\sum Y_i^2} = 1 - \frac{\text{residual sum of squares}}{\text{uncorrected sum of squares (USS)}} = 1 - \frac{\text{deviance}}{\text{USS}}$$

$$AIC_c = AIC + \frac{2K(K+1)}{n-K-1}$$

where K is the number of parameters in a model and *n* is the number of observations

Figure	Model	N_c	*t*-test results		Fit statistics				
			β1	β2	RMSE	Error d.f.	MAE	AIC$_c$	R^2
2*a*	$\tan A = 1.190 N_c^{-1/2}$	<10	Y		0.1665	12	0.097	−5.55	0.956
	$\tan A = 1.044 N_c^{-1/3}$	<10	Y		0.1352	12	0.094	−10.98	0.971
	$\tan A = 3.931 N_c^{-2/3}$	>10	Y		0.0839	8	0.060	−14.12	0.977
2*b*	$\tan A = 4.458 N_c^{-2/3}$	>10	Y		0.2578	13	0.189	5.83	0.862
	$\tan A = 4.119 N_c^{-2/3}$, outlier removed	>10	Y		0.1927	12	0.155	−1.77	0.906
	$\tan A = 1.041 N_c^{-1/3}$, outlier removed	<10	Y		0.1896	17	0.139	−5.02	0.916
	$\tan A = 0.655 N_c^{-0.03}$, outlier removed	All N_c	Y	N	0.1341	29	0.095	−31.77	0.956
3*a*	$F_H = 2.421 N_c^{-1}$	>10	Y		0.0157	8	0.013	−44.31	0.985
	$F_H = 1.676 N_c^{-1}$	<10	Y		0.1464	12	0.092	−8.90	0.966
	$F_H = 1.726 N_c^{-1.04}$	All N_c	Y	Y	0.1159	20	0.071	−27.16	0.965
3*b*	$F_H = 2.310 N_c^{-1}$	>10	Y		0.0408	13	0.031	−45.22	0.913
	$F_H = 1.362 N_c^{-1}$	<10	Y		0.1480	17	0.106	−13.94	0.845
	$F_H = 1.397 N_c^{-1}$	All N_c	Y		0.1178	31	0.082	−42.65	0.837
	$F_H = 0.878 N_c^{-0.62}$	All N_c	Y	Y	0.0932	30	0.060	−56.30	0.901
4*a*	$H = 0.0024 I_B u_a^{-1}$	>10	Y		0.0947	8	0.073	−11.95	0.973
	$H = 0.0033 I_B u_a^{-1}$	<10	Y		0.1076	12	0.0784	−12.75	0.968
4*b*	$H = 0.0024 I_B u_a^{-1}$, outliers removed	>10	Y		0.3342	11	0.270	12.04	0.955
	$H = 0.0035 I_B u_a^{-1}$, outliers removed	<10	Y		0.5514	16	0.362	31.83	0.943
5*a*	$H = 0.0173 I_B^{2/3}$	>10	Y		0.1223	8	0.096	−7.34	0.954
	$H = 0.0132 I_B^{2/3}$	<10	Y		0.1248	12	0.094	−13.06	0.958
	$H = 0.0142 I_B^{2/3}$	All N_c	Y		0.1405	21	0.105	−20.32	0.941
5*b*	$H = 0.0155 I_B^{2/3}$, outlier removed	All N_c	Y		0.5445	26	0.392	47.27	0.931

International Journal of Wildland Fire ©IAWF 2012
doi:10.1071/WF10034_AC

Accessory publication

Entrainment regimes and flame characteristics of wildland fires

Ralph M. Nelson Jr[A,D], *Bret W. Butler*[B] *and David R. Weise*[C]

[A]US Forest Service, 206 Morning View Way, Leland, NC 28451, USA. [Retired].

[B]US Forest Service, Rocky Mountain Research Station, Missoula Fire Sciences Laboratory, Missoula, MT 59807, USA.

[C]US Forest Service, Southwest Research Station, Forest Fire Laboratory, Pacific Riverside, CA 92507, USA.

[D]Corresponding author. Email: nelsonsally@bellsouth.net

Herein we report details of the derivation of two supplementary flame characteristic models and a discussion of flame tilt angle in the laboratory and field for which space was not available in the published text.

Background

In the published text, equations for entrainment parameters and flame characteristics of steadily burning 2-D head fires in uniform wildland fuels are derived. The text suggests three separate regimes of flow above such fires, with two of these regimes delineated by a critical value of the Byram convection number $N_c = 10$. The starting point for the flame characteristic derivations is a simplified version of the Albini (1981) flame model. The model equations are tested with fire behaviour data from laboratory wind tunnel burns in slash pine litter fuels (Nelson and Adkins 1986) and field data reported in Appendix A of the text. It is shown that flame characteristics derived from the Albini model are descriptive of flame tilt angle only in the laboratory fires and, as expected, only when $N_c < 10$. The authors wish to present alternative flame angle models for the $N_c > 10$ regime to give the reader a complete report of our work and provide modeling approaches that bring the models into agreement with the experimental data.

tan*A* in laboratory and field fires for $N_c > 10$

The sketch in Fig. 1 of the text depicts a time-averaged visible flame of height H tilted at mean angle A from vertical; the flame shape approximates a rectangular solid with flow area A_f (thickness $D_o\cos A$ by unit width L of fireline into the page) and length $H\sec A$. A mixture of burning volatiles and combustion-zone air flows steadily along the flame axis with a velocity whose 'whole fire' mean vertical component (rather than vertical velocity w at z) is the characteristic velocity w_c (Eqn 18 of the text). The mean flame temperature of 750 K ((1000 +

500)/2) is computed from previously assumed values for T_o and T_t. We assume that viscous forces are negligible and the fluid is incompressible (mean density ρ_c = 0.48 kg m^{-3}); thus, the integrated form of the Euler equation (Lay 1964) may be used to write the vertical buoyant force as

$$F_B = -A_f \Delta p = gD_o \cos A(\rho_a - \rho_c)HL \sec A = \left(\frac{\rho_c w_c^2}{2}\right)HL \quad \text{(A1)}$$

where Δp is the pressure drop in the flame due to buoyancy. The horizontal drag force on the flame, using Eqn 19 of the text, is

$$F_D = \frac{C_D \rho_a u_e^2 A_p}{2} = \frac{C_D}{2}\rho_a \eta^2 u_a^2 HL \quad \text{(A2)}$$

where C_D is the drag coefficient for the inclined flame and A_p is the projected area (the area normal to the direction of air flow). The balance of transverse forces that determines angle A is $F_B \sin A = F_D \cos A$ and leads to

$$\tan A = \frac{F_D}{F_B} = \frac{C_D \rho_a \eta^2 u_a^2}{\rho_c w_c^2} = 3.85\eta^2 N_c^{-2/3} \quad \text{(A3)}$$

where C_D = 1.54 (Fang 1969).

Differences in tan*A* data for laboratory and field fires

Fig. 2 of the text indicates that tan$A$ relationships for the laboratory and field fires differ significantly. For the laboratory fires, tan$A$ is proportional to either $N_c^{-1/2}$ or $N_c^{-1/3}$ when $N_c < 10$, and follows Eqn A3 when $N_c > 10$. In the field, tan$A$ is constant for all N_c. These differing results may be related to hindered *v.* freely moving combustion products in and above the flame for the laboratory and field fires respectively. We expect smaller tilt angles and reciprocal N_c values in field measurements than would be observed for the same fire in a wind tunnel. In the field, the reduced influence of wind speed and tilt angle should combine with generally greater fuel loads and an increased rate of spread due to greater fireline length (Cheney and Sullivan 1997) to drive tan$A$ toward a constant value. The dependence of tan$A$ on powers of N_c close to –1/3 seems associated with fires in wind tunnels with fixed ceilings (Taylor 1961; Nelson and Adkins 1986); an exception is the study of Weise and Biging (1996) who found a dependence close to $N_c^{-1/3}$ even though their relatively small tunnel was operated with a moving ceiling. However, a tendency toward N_c independence, or at most a weak dependence, seems to occur in relatively large wind tunnels (Anderson *et al.* 2006) and in tunnels that allow free convection (Fendell *et al.* 1990).

tan*A* in the field fires based on kinetic energy flux

We assume the flame tilt angle is determined by a balance between the transverse components of the kinetic energy flux of ambient air approaching the flame and the vertical flame fluid kinetic energy flux due to buoyancy. This balance is given by:

$$(\mathrm{d}W/\mathrm{d}t)_{\mathrm{drag}} = (\mathrm{d}W/\mathrm{d}t)_{\mathrm{buoyancy}} = F_D u_e \cos A = F_B w_c \sin A$$

where W is work done and t is time. With this interpretation, rates at which parcels of air and flame fluid do work apparently govern flame tilt angle for moderate winds in the field, whereas a mass flux balance is operative in wind tunnels such as the SFFL tunnel in which the steady winds are more unidirectional because convection is confined. Use of Eqns 20 of the text and A1 and A2 above leads to

$$\tan A = C_D \rho_a \alpha^3 / \rho_c = 3.85\alpha^3 \quad \text{(A4)}$$

This equation gives an estimate of entrainment constant α identical to that derived for the lab fires from Eqn 23 of the text.

References

Albini FA (1981) A model for the wind-blown flame from a line fire. *Combustion and Flame* **43**, 155–174. doi:10.1016/0010-2180(81)90014-6

Anderson W, Pastor E, Butler B, Catchpole E, Dupuy JL, Fernandes P, Guijarro M, Mendes-Lopes JM, Ventura J (2006) Evaluating models to estimate flame characteristics for free-burning fires using laboratory and field data. In 'Proceedings, V International Conference on Forest Fire Research', 27–30 November 2006, Figueira da Foz, Portugal. (Ed. DX Viegas). (CD-ROM) (Elsevier BV: Amsterdam)

Cheney P, Sullivan A (1997) 'Grassfires: fuel, weather and fire behaviour.' (CSIRO Publishing: Melbourne)

Fang JB (1969) An investigation of the effect of controlled wind on the rate of fire spread. PhD thesis, University of New Brunswick, Fredericton, NB.

Fendell FE, Carrier GF, Wolff MF (1990) Wind-aided fire spread across arrays of discrete fuel elements. US Department of Defense, Defense Nuclear Agency, Technical Report DNA-TR-89–193. (Alexandria, VA)

Lay JE (1964) 'Thermodynamics: a macroscopic-microscopic treatment.' (Charles E Merrill Books, Inc.: Columbus, OH)

Nelson RM Jr, Adkins CW (1988) A dimensionless correlation for the spread of wind-driven fires. *Canadian Journal of Forest Research* **18**, 391–397. doi:10.1139/x88-058

Taylor GI (1961) Fire under the influence of natural convection. In 'The use of models in fire research'. (Ed. WG Berl) National Academy of Science, National Research Council Publication 786, pp. 10–32. (Washington, DC)

Weise DR, Biging GS (1996) Effects of wind velocity and slope on flame properties. *Canadian Journal of Forest Research* **26**, 1849–1858. doi:10.1139/x26-210

International Journal of Wildland Fire ©IAWF 2012
doi:10.1071/WF10034_AC

Accessory publication

Entrainment regimes and flame characteristics of wildland fires

Ralph M. Nelson Jr[A,D], *Bret W. Butler*[B] *and David R. Weise*[C]

[A]US Forest Service, 206 Morning View Way, Leland, NC 28451, USA. [Retired].

[B]US Forest Service, Rocky Mountain Research Station, Missoula Fire Sciences Laboratory, Missoula, MT 59807, USA.

[C]US Forest Service, Southwest Research Station, Forest Fire Laboratory, Pacific Riverside, CA 92507, USA.

[D]Corresponding author. Email: nelsonsally@bellsouth.net

Herein we report details of the derivation of two supplementary flame characteristic models and a discussion of flame tilt angle in the laboratory and field for which space was not available in the published text.

Background

In the published text, equations for entrainment parameters and flame characteristics of steadily burning 2-D head fires in uniform wildland fuels are derived. The text suggests three separate regimes of flow above such fires, with two of these regimes delineated by a critical value of the Byram convection number $N_c = 10$. The starting point for the flame characteristic derivations is a simplified version of the Albini (1981) flame model. The model equations are tested with fire behaviour data from laboratory wind tunnel burns in slash pine litter fuels (Nelson and Adkins 1986) and field data reported in Appendix A of the text. It is shown that flame characteristics derived from the Albini model are descriptive of flame tilt angle only in the laboratory fires and, as expected, only when $N_c < 10$. The authors wish to present alternative flame angle models for the $N_c > 10$ regime to give the reader a complete report of our work and provide modeling approaches that bring the models into agreement with the experimental data.

tan*A* in laboratory and field fires for $N_c > 10$

The sketch in Fig. 1 of the text depicts a time-averaged visible flame of height *H* tilted at mean angle *A* from vertical; the flame shape approximates a rectangular solid with flow area A_f (thickness $D_o\cos A$ by unit width *L* of fireline into the page) and length $H\sec A$. A mixture of burning volatiles and combustion-zone air flows steadily along the flame axis with a velocity whose 'whole fire' mean vertical component (rather than vertical velocity *w* at *z*) is the characteristic velocity w_c (Eqn 18 of the text). The mean flame temperature of 750 K ((1000 +

500)/2) is computed from previously assumed values for T_o and T_t. We assume that viscous forces are negligible and the fluid is incompressible (mean density ρ_c = 0.48 kg m^{-3}); thus, the integrated form of the Euler equation (Lay 1964) may be used to write the vertical buoyant force as

$$F_B = -A_f \Delta p = gD_o \cos A(\rho_a - \rho_c)HL \sec A = \left(\frac{\rho_c w_c^2}{2}\right)HL \quad \text{(A1)}$$

where Δp is the pressure drop in the flame due to buoyancy. The horizontal drag force on the flame, using Eqn 19 of the text, is

$$F_D = \frac{C_D \rho_a u_e^2 A_p}{2} = \frac{C_D}{2}\rho_a \eta^2 u_a^2 HL \quad \text{(A2)}$$

where C_D is the drag coefficient for the inclined flame and A_p is the projected area (the area normal to the direction of air flow). The balance of transverse forces that determines angle A is $F_B \sin A = F_D \cos A$ and leads to

$$\tan A = \frac{F_D}{F_B} = \frac{C_D \rho_a \eta^2 u_a^2}{\rho_c w_c^2} = 3.85\eta^2 N_c^{-2/3} \quad \text{(A3)}$$

where C_D = 1.54 (Fang 1969).

Differences in tan*A* data for laboratory and field fires

Fig. 2 of the text indicates that tan$A$ relationships for the laboratory and field fires differ significantly. For the laboratory fires, tan$A$ is proportional to either $N_c^{-1/2}$ or $N_c^{-1/3}$ when $N_c < 10$, and follows Eqn A3 when $N_c > 10$. In the field, tan$A$ is constant for all N_c. These differing results may be related to hindered *v.* freely moving combustion products in and above the flame for the laboratory and field fires respectively. We expect smaller tilt angles and reciprocal N_c values in field measurements than would be observed for the same fire in a wind tunnel. In the field, the reduced influence of wind speed and tilt angle should combine with generally greater fuel loads and an increased rate of spread due to greater fireline length (Cheney and Sullivan 1997) to drive tan$A$ toward a constant value. The dependence of tan$A$ on powers of N_c close to −1/3 seems associated with fires in wind tunnels with fixed ceilings (Taylor 1961; Nelson and Adkins 1986); an exception is the study of Weise and Biging (1996) who found a dependence close to $N_c^{-1/3}$ even though their relatively small tunnel was operated with a moving ceiling. However, a tendency toward N_c independence, or at most a weak dependence, seems to occur in relatively large wind tunnels (Anderson *et al.* 2006) and in tunnels that allow free convection (Fendell *et al.* 1990).

tan*A* in the field fires based on kinetic energy flux

We assume the flame tilt angle is determined by a balance between the transverse components of the kinetic energy flux of ambient air approaching the flame and the vertical flame fluid kinetic energy flux due to buoyancy. This balance is given by:

$$(\mathrm{d}W/\mathrm{d}t)_{\mathrm{drag}} = (\mathrm{d}W/\mathrm{d}t)_{\mathrm{buoyancy}} = F_D u_e \cos A = F_B w_c \sin A$$

where W is work done and t is time. With this interpretation, rates at which parcels of air and flame fluid do work apparently govern flame tilt angle for moderate winds in the field, whereas a mass flux balance is operative in wind tunnels such as the SFFL tunnel in which the steady winds are more unidirectional because convection is confined. Use of Eqns 20 of the text and A1 and A2 above leads to

$$\tan A = C_D \rho_a \alpha^3 / \rho_c = 3.85\alpha^3 \quad \text{(A4)}$$

This equation gives an estimate of entrainment constant α identical to that derived for the lab fires from Eqn 23 of the text.

References

Albini FA (1981) A model for the wind-blown flame from a line fire. *Combustion and Flame* **43**, 155–174. doi:10.1016/0010-2180(81)90014-6

Anderson W, Pastor E, Butler B, Catchpole E, Dupuy JL, Fernandes P, Guijarro M, Mendes-Lopes JM, Ventura J (2006) Evaluating models to estimate flame characteristics for free-burning fires using laboratory and field data. In 'Proceedings, V International Conference on Forest Fire Research', 27–30 November 2006, Figueira da Foz, Portugal. (Ed. DX Viegas). (CD-ROM) (Elsevier BV: Amsterdam)

Cheney P, Sullivan A (1997) 'Grassfires: fuel, weather and fire behaviour.' (CSIRO Publishing: Melbourne)

Fang JB (1969) An investigation of the effect of controlled wind on the rate of fire spread. PhD thesis, University of New Brunswick, Fredericton, NB.

Fendell FE, Carrier GF, Wolff MF (1990) Wind-aided fire spread across arrays of discrete fuel elements. US Department of Defense, Defense Nuclear Agency, Technical Report DNA-TR-89–193. (Alexandria, VA)

Lay JE (1964) 'Thermodynamics: a macroscopic-microscopic treatment.' (Charles E Merrill Books, Inc.: Columbus, OH)

Nelson RM Jr, Adkins CW (1988) A dimensionless correlation for the spread of wind-driven fires. *Canadian Journal of Forest Research* **18**, 391–397. doi:10.1139/x88-058

Taylor GI (1961) Fire under the influence of natural convection. In 'The use of models in fire research'. (Ed. WG Berl) National Academy of Science, National Research Council Publication 786, pp. 10–32. (Washington, DC)

Weise DR, Biging GS (1996) Effects of wind velocity and slope on flame properties. *Canadian Journal of Forest Research* **26**, 1849–1858. doi:10.1139/x26-210